jove

Activity of Posterior Lateral Line Afferent Neurons during Swimming in Zebrafish

Elias T. Lunsford[1], **James C. Liao**[1]

[1] Department of Biology, University of Florida, The Whitney Laboratory for Marine Bioscience

Corresponding Author

James C. Liao
jliao@whitney.ufl.edu

Citation

Lunsford, E.T., Liao, J.C. Activity of Posterior Lateral Line Afferent Neurons during Swimming in Zebrafish. *J. Vis. Exp.* (168), e62233, doi:10.3791/62233 (2021).

Date Published

February 10, 2021

DOI

10.3791/62233

URL

jove.com/video/62233

Abstract

Sensory systems gather cues essential for directing behavior, but animals must decipher what information is biologically relevant. Locomotion generates reafferent cues that animals must disentangle from relevant sensory cues of the surrounding environment. For example, when a fish swims, flow generated from body undulations is detected by the mechanoreceptive neuromasts, comprising hair cells, that compose the lateral line system. The hair cells then transmit fluid motion information from the sensor to the brain via the sensory afferent neurons. Concurrently, corollary discharge of the motor command is relayed to hair cells to prevent sensory overload. Accounting for the inhibitory effect of predictive motor signals during locomotion is, therefore, critical when evaluating the sensitivity of the lateral line system. We have developed an in vivo electrophysiological approach to simultaneously monitor posterior lateral line afferent neuron and ventral motor root activity in zebrafish larvae (4-7 days post fertilization) that can last for several hours. Extracellular recordings of afferent neurons are achieved using the loose patch clamp technique, which can detect activity from single or multiple neurons. Ventral root recordings are performed through the skin with glass electrodes to detect motor neuron activity. Our experimental protocol provides the potential to monitor endogenous or evoked changes in sensory input across motor behaviors in an intact, behaving vertebrate.

Introduction

Afferent neurons of mechanosensory systems transmit information from hair cells to the brain during hearing and balance. Electrophysiology can reveal the sensitivity of afferent neurons through direct recordings. While whole cell patching from hair cells can be challenging, recording from downstream afferent neurons is easier and allows assessment of action potentials in response to controlled stimulations[1,2,3]. Stimulating hair cells lead to their deflection, which modifies mechanosensory structures, thus triggering an increase in action potentials (spikes) in afferent neurons[4,5,6]. In the absence of external stimuli, afferent neurons also spike spontaneously due to glutamate leak

from the hair cells on to afferent post-synaptic terminals[7,8], and have been shown to contribute toward maintaining sensitivity[9,10]. Patch clamp recording of afferent activity enables observation of hair cell sensitivity and signal dynamics that are not possible using techniques with lower temporal resolution, such as in microphonics[11,12] or functional calcium imaging[13,14,15]. The following protocol will allow the recording of afferent activity concurrent with motor commands to reveal instantaneous changes in hair cell sensitivity.

Zebrafish (*Danio rerio*) use hair cells contained in neuromasts that compose the lateral line system to detect water movement relative to their body, which is translated into neural signals essential for navigation[16,17,18], predator avoidance, prey capture[19,20], and schooling[21]. Water flow can also be self-generated by the motions of swimming[22,23,24], respiration[22,25,26], and feeding[27]. These behaviors comprise repetitive movements that can fatigue hair cells and impair sensing. Therefore, it is critical that the lateral line system differentiates between external (exafferent) and self-generated (reafferent) flow stimuli. A corollary discharge attenuates self-generated flow signals during locomotion in zebrafish. This inhibitory predictive motor signal is relayed via descending neurons to the sensory receptors to modify the input or interrupt the processing of the reafferent feedback[28,29]. Seminal work contributing to our early understanding of this feedforward system relied on in vitro preparations where the connectivity and endogenous activity of the neural circuit were not maintained[28,30,31,32,33,34,35]. This protocol describes an approach to preserving an intact neural circuit where endogenous feedback dynamics are maintained thus enabling better understanding of the corollary discharge in vivo.

The protocol outlined here describes how to monitor posterior lateral line afferent neuron and motor neuron activity simultaneously in larval zebrafish. Characterizing afferent signal dynamics before, during, and after motor commands provides insights into real-time, endogenous feedback from the central nervous system that modulates hair cell sensitivity during locomotion. This protocol outlines what materials will need to be prepared prior to experiments and then describes how to paralyze and prepare zebrafish larvae. The protocol will describe how to establish a stable loose patch recording of afferent neurons and extracellular ventral root (VR) recordings of motor neurons. Representative data that can be obtained using this protocol are presented from an exemplar individual and analysis was performed on multiple replicates of the experimental protocol. Pre-processing of data is performed using custom written scripts in MATLAB. Overall, this in vivo experimental paradigm is poised to provide a better understanding of sensory feedback during locomotion in a model vertebrate hair cell system.

Protocol

All animal care and experiments were performed in accordance with protocols approved by the University of Florida's Institutional Animal Care and Use Committee.

1. Preparation of materials for electrophysiological recordings

1. Make a silicone elastomer-bottomed recording dish.
    1. Dispense a thin layer of self-mixing silicone elastomer components (e.g., Sylgard) into a cover glass bottomed tissue culture dish until it levels with

the rim of shallow well. Approximately 0.5 mL is sufficient.

2. Cover and cure the dish for a minimum of 48 h at room temperature.

2. Make dissection pins.

1. Provide a negative charge (5 V) to a 100 mL beaker of etchant (3M KOH) using a DC power supply and attach a tungsten wire (0.002 inch; 50.8 µm diameter) to the positively charged output.
CAUTION: Negative and positive wires should not contact one another during this procedure as you may run the risk of producing sparks, which could pose a potential fire hazard.

2. Etch tungsten wire by quickly and repeatedly dipping the tip of the wire into the etchant bath until the tip narrows to a sharp point. Under a stereomicroscope, cut the wire approximately 1 mm from the tip with a straight edge razor blade. Repeat three more times and then insert pins into cured recording dish using fine forceps.

3. Prepare recording electrodes.

1. Pull a borosilicate glass capillary tube (inner diameter: 0.86 mm, outer diameter: 1.50 mm) using a horizontal micropipette puller with box filament into electrodes with a 30 µm diameter tip with slight taper (**Figure 1 Ai**) that will be used to record afferent neurons from the posterior lateral line.

2. Pull an additional borosilicate glass capillary tube into a pair of electrodes with smaller tip diameters (1-5 µm). Holding one electrode in each hand, gently run the tips across one another to break them to a ~30° angle. Using a microforge, polish the beveled tip until smooth. The final tip diameter should be between 30-50 µm and will be used as the ventral root (VR) recording electrode (**Figure 1 Aii**).

3. Mark the side of the VR electrode with the leading edge with permanent ink to aid in orienting the tip aperture downward when inserting the electrode into the pipette holder of the headstage (step 3.2).
NOTE: Mechanical modification of the VR recording electrode is imprecise and step 1.3.2 may require multiple attempts until a suitable tip morphology is attained before polishing. VR recording electrode is beveled to conform to the body curve of the larvae. Once fabricated, the VR recording electrode can be used repeatedly as long as the tip remains clear and clean between experiments.

4. Generate the protocol in electrophysiology recording programs.

1. Ensure the right headstage is connected to the **Channel 1** input in the back of the microelectrode current and voltage clamp amplifier for the afferent neuron recordings and the left headstage is connected to the **Channel 2** input for the VR recordings.
NOTE: Computer specifications for the current and voltage clamp amplifier minimally require 1 Ghz or a better processor, Windows XP Pro or Mac OS X 10.46.6, CD-ROM drive with 512 MB RAM, 500 MB hard drive space, and 2 USB ports.

2. Open the computer-controlled amplifier software.

3. Set **Channel 1** and **Channel 2** to current clamp mode by clicking the **IC** button for each channel.

4. Input the following parameters under both **I-Clamp 1** and **I-Clamp 2** tabs . **Primary Output:** 100x AC Membrane Potential (100,000 mV/mV), **Gain**: 1,000,

Bessel: 1 kHz , **AC**: 300 Hz , **Scope**: Bypass . **Secondary Output:** 100x AC Membrane Potential (100 mV/mV) , **Gain**: 1 , **Lowpass Filter:** 10 Hz.

5. Save channel parameters as **Ch1_Aff** and **Ch2_VR**.
6. Install and open the patch clamp electrophysiology software.
7. Click on **Configure** and select **Lab Bench** to set up the analog signals by adding **Ch1_Aff** and **Ch2_Vr** to **Digitizer Channels** (e.g., **Analog IN #0** and **Analog IN #1**) that are connected, by BNC coaxial cable, to the corresponding **Channel 1** and **Channel 2 Scaled Outputs** of the amplifier. Click on **OK**.
   NOTE: The minimum computer requirements for the digitizer are: a 1 Ghz or better processor, Windows XP Pro or Mac OS X 10.46.6, CD-ROM drive 512 MB RAM, 500 MB hard drive space, and 2 USB ports.
8. Click on **Acquire** and select **New Protocol**.
9. In the **Mode/Rate** tab, select **Gap Free**; under **Acquisition Mode**, set **Trial Length** to either **Use available disk space** (i.e., record until stopped) or a desired set **Duration (hh:mm:ss)**, and then set the **Sampling rate per signal (Hz)** to **20,000** to maximize the resolution.
10. Under the **Inputs** tab, select the **Analog IN Channels** that were previously configured (in step 1.4.6) and select **Ch1_Aff** and **Ch2_VR** for the corresponding channel.
11. Under the **Outputs** tab, select **Cmd 0** and **Cmd 1** for **Channel #0** and **Channel #1**, respectively.
    1. Connect Channel 1 Command on the amplifier to Analog Ouput 0 on the digitizer via BNC coaxial cable and repeat for Channel 2 Command to Analog Output 1.
12. The remaining tabs can remain under default settings. Click on **OK** and save the protocol.

2. Solution preparation

1. Prepare Hank's solution: 137 mM NaCL, 5.4 mM KCl, 0.25 mM Na_2HPO_4, 0.44 mM KH_2PO_4, 1.3 mM $CaCl_2$, 1.0 mM $MgSO_4$, 4.2 mM $NaHCO_4$; pH 7.3. Dilute to 10% Hank's solution by adding the appropriate volume of deionized water to the stock.
2. Prepare extracellular solution: 134 mM NaCl, 2.9 mM KCl, 1.2 mM $MgCl_2$, 2.1 mM $CaCl_2$, 10 mM glucose, 10 mM HEPES buffer; pH 7.8 adjusted with NaOH. Vacuum filter extracellular solution through the filter with 0.22 µm pore size.
3. Prepare α -bungarotoxin: Dissolve 1 mg of lyophilized α-bungarotoxin in 10 mL extracellular solution to produce 0.1% dilution.
4. Prepare Euthanasia solution: 50% (mg/L) buffered pharmaceutical-grade MS-222 in 10% Hank's solution.
   CAUTION: α-bungarotoxin is a potent neurotoxin that paralyzes muscles by blocking cholinergic receptors. Gloves are required and eye protection is recommended while handling the paralytic.

3. Preparation of larvae for electrophysiological recordings

1. Immobilize zebrafish larvae.
   1. Use larvae from the laboratory-bred population of zebrafish (*Danio rerio*; 4-7 days post fertilization) and house in embryo solution (10% Hank's solution) at 27 °C.

2. Transfer larva from housing into a small Petri dish (35 mm) using a large-tipped transfer pipette and remove as much of the surrounding solution as possible.

   NOTE: Removal of the embryo solution prevents dilution of the paralytic and increases its efficacy. The corner of a task wipe can be used to wick away the remaining embryo solution, and it is critical not to contact the larvae or leave larvae exposed to air.

3. Immerse larvae in 10 µL of 0.1% α-bungarotoxin for approximately 5 min.

   NOTE: The time necessary to immobilize larvae varies between preparations. A healthy preparation depends on closely monitoring sustained fast blood flow and decreased motor responses. Brief overexposure to the paralytic can lead to a slow decline in overall health of the preparation even after a thorough washout. It is best to apply a wash before the larva is completely immobilized while it still shows signs of subtle muscle vibrations.

4. Wash paralyzed larva with extracellular solution and bathe for 10 min.

   NOTE: The washout allows for the larva to transition from subtle muscle vibrations to complete paralysis. Also, α-bungarotoxin is an antagonist of the nicotinic acetylcholine receptor (nAChR) α9-subunit, which is a critical component of the endogenous feedback circuit this protocol observes; however, this effect has been shown to be reversible in *Xenopus* and zebrafish hair cells after a 10 min washout[36,29].

2. Pin fish in the recording dish.

   NOTE: Anesthesia (e.g., MS-222, Tricaine) is not required while preparing larval zebrafish (4-7 dpf) as it interferes with animal health. In fact, larval zebrafish are exempt from certain vertebrate protocols.

1. Using transfer pipette, move the larva from the extracellular solution bath to the silicone-bottomed recording dish. Fill the remainder of the dish with extracellular solution.

2. Under a stereomicroscope, gently position the larvae with fine-tipped forceps above the center of the silicone mat, lateral side up, with the body's anterior and posterior ends running left to right, respectively. Then grasp an etched pin from the silicone mat using fine-tipped forceps and insert the pin, orthogonally to the silicone, through the dorsal notochord of the larvae directly dorsal to the anus. Insert the second pin through the notochord near the end of the tail and insert the third pin through the notochord dorsal of the gas bladder (**Figure 1B**).

   NOTE: While inserting pins, it is important to target the center of the notochord width to prevent impinging blood flow or damaging surrounding musculature. The notochord is dorsal to the posterior lateral line nerve, so with proper pinning, no damage is expected to the lateral line sensory neurons. Insert after first contact as to not disturb the surrounding tissue. Ideally, the diameter of the pin is less than half the width of the notochord to ensure clean insertion. If the pins exceed this width, repeat step 1.2 until the desired pin width is attained. If the blood flow slows after pinning, repeat from step 1.3 onward with a new specimen.

3. Insert the fourth pin through the otic vesicle while providing slight rotation towards the anterior as the pin inserts into the encapsulant (**Figure 1B**). As a slight rotation is applied, watch for the tissue

between the cleithrum and otic vesicle to reveal the cluster of afferent somata.

NOTE: Angled insertion of the fourth pin is to ensure the exposure of the posterior lateral line afferent ganglion, which is otherwise obstructed by the large otic vesicle.

4. Ventral root recording

1. Place pinned larva under the 10x water immersion objective on a fixed stage differential interference contrast (DIC) upright microscope and orient the myseptal clefts of the muscle blocks parallel to the left headstage approach vector (**Figure 1B**).
    1. A fixed stage DIC microscope floated on an optical air table works best to prevent vibrations from interfering with the recordings. Using a motorized positioner, the microscope can then move freely around the fixed stage in which the preparation and headstages are mounted (**Figure 1C**).
    2. Place the ground wire into the bath solution and ensure that it is connected to the left headstage.
2. Fill the VR recording electrode with 30 µL of extracellular solution using a flexible gel-loading pipette tip and insert into the left headstage pipette holder.
3. Lower the recording pipette into the dish solution with a micromanipulator while applying positive pressure (1-2 mmHg) produced by a pneumatic transducer. Under 10x magnification, confirm the orientation of the tip aperture is facing downward.
    1. The pneumatic transducer should be connected to the pipette holder port via silicone tubing.
4. Place the VR electrode onto the myoseptum
    1. Using the micromanipulator again, lower the VR electrode tip until it is holding position above the larva. Increase the magnification to 40x immersion.
    2. Bring the electrode tip over a myoseptum between two myomeres ventral to the lateral line until the cleft is centered in the VR electrode tip aperture (**Figure 1D**).
    3. Lower the pipette until the lagging edge of the tip aperture gently contacts the epithelium. After initial contact, maneuver the pipette diagonally to ensure the leading edge makes contact and can generate a seal.
    4. Apply negative pressure (~100 mm Hg) with the pneumatic transducer and hold.

    NOTE: Proper orientation of the VR pipette relative to the myoseptum and continuous negative pressure optimizes detecting motor neuron activity with a high signal-to-noise ratio through the skin.
5. Detect motor neuron activity.
    1. The left headstage should be connected to the amplifier, which relays the amplified signal into a digitizer that outputs the said signal into the patch clamp electrophysiology software to be monitored on an adjacent computer (see section 1.4).
    2. In the patch clamp software, click on the Play button on the tool bar to monitor the VR signal (**Figure 1E**).
    3. Ensure that the VR recording is being achieved once motor neuron activity with well-stereotyped burst signal dynamics are observed[29,37] (**Figure 1E**).

    NOTE: Fictive swim bouts are the activity patterns of the VR motor neurons that continue to transmit despite the preparation being paralyzed.

Therefore, fictive swims are an accessible means of determining the behavioral state of the animal and measuring locomotor parameters while simultaneously performing afferent neuron recordings that require an immobilized preparation. In our hands, once a VR recording is achieved, a healthy preparation will elicit voluntary fictive swim bouts every few seconds. Remember, a healthy preparation has sustained fast blood flow. Be advised, obtaining a sufficient VR signal may take several minutes and the signal-to-noise ratio may improve after initial detection. In the interest of time, it is acceptable to move on to section 5.

4. If a VR recording is still not achieved after completing section 5, release negative pressure, raise the electrode, and repeat from step 4.4.2 onward on a different myoseptum if the larva health is still optimal.

5. Afferent neuron recording

1. Fill the afferent recording electrode with 30 µL of extracellular solution; insert into the right headstage pipette holder (**Figure 1B,C**), and lower into the dish solution while applying positive pressure (1-2 mm Hg) produced by a pneumatic transducer.
2. Locate and loosely attach to posterior lateral line afferent ganglion.
    1. Using a micromanipulator, lower the afferent electrode tip until it is holding position above the cleithrum.
    2. Increase the magnification to 40x immersion and locate the intersection of the posterior lateral line nerve and cleithrum. Follow the lateral line nerve anterior from the cleithrum to where the fibers innervate the posterior lateral line afferent ganglion, distinguishable by the discrete cluster of soma (**Figure 1F**).
    3. Bring the electrode tip over the afferent ganglion and lower the pipette until the tip contacts the epithelium. Gently, maneuver the electrode so that the entire tip circumference contacts the afferent ganglion.
    4. Apply negative pressure (20-50 mm Hg) with the pneumatic transducer and hold.
    NOTE: The negative pressure applied to the afferent ganglion is gentler than the suction applied during the ventral root recording. Increasing negative pressure can improve signal-to-noise, but afferent neuron health declines under sustained aggressive suction, which decreases the probability of a successful recording.
3. Record afferent neuron activity.
    1. Ensure that the right headstage is connected in a similar sequence as described in step 4.5.1.
    2. In pClamp10, click on the **Play** button on the tool bar to monitor afferent neuron and VR signal simultaneously.
    3. Ensure that the whole cell, loose patch recording of afferent neurons is achieved once spikes occur spontaneously, roughly every 100-200 ms[1,29] (**Figure 1E**).
    4. Gradually, increase the afferent neuron recording electrode pressure back to atmospheric (0 mm Hg) and hold for the remainder of the recording.

6. Data acquisition

1. Simultaneous recording.

1. Once afferent neuron and motor neuron activity are both detected, click on the **Record** button on the tool bar in pClamp10 to capture simultaneous gap free recordings in both the channels.
2. Record for the desired duration (**Figure 1E**).
   NOTE: A recording in a healthy preparation can last for many hours and remain responsive to external stimuli.
3. Save the recording as a supported file type (.abf, pClamp10) to preserve metadata such as acquisition parameters.

7. Euthanasia

1. Apply positive pressure (10 mm Hg) to both afferent and VR recording electrodes using pneumatic transducers and raise the electrodes from the recording dish using the micromanipulators.
2. Transfer the recording dish from the fixed stage DIC microscope to the dissection stereomicroscope.
3. Using fine tip forceps, remove tungsten pins from notochord and otic capsule, and transfer the larvae using a transfer pipette into a Petri dish (35 mm) containing 5 mL of euthanasia solution for a minimum of 5 min.

8. Pre-processing and data-analysis

NOTE: Data pre-processing and analysis will require a basic understanding of command line coding.

1. Convert the recording file for pre-processing.
   1. Install the Matlab software.
   2. Download the custom written script, abfload.m[38] and save the file into the same folder that stores the raw recording file.
   3. In the **Matlab Editor** window, open abfload.m and click on **Run** on the tool bar. Select **Change Folder**, if prompted.
   4. Execute the function in the **Command Window** with the raw recording file as the input,
      > [d,si,h] = **abfload**('[raw recording file name].abf')
      and save the output workspace with a file name that includes larva designation, age, and experimental date such as [specimen number]_[age in dpf]_[raw recording file name (includes experimental date by default)].
      NOTE: The converted file name should only include underscore delineated integers.
2. Perform data pre-processing.
   1. Download Matlab script AffVR_preprocess.m and associated functions, custom written by the authors.
   2. In the **Editor** window, open AffVR_preprocess.m.
   3. Under **Variables**, adjust lower bound spike detection thresholds for both afferent and VR recordings (**spk_detect_lb** and **vr_detect_lb**, lines 8 and 14, respectively) depending on the recording of the signal-to-noise ratio.
      NOTE: Spike detection relies on manual thresholding to sort and isolate signals from more than one afferent neuron by amplitude. Baseline noise and activity from other units are filtered out by thresholding to only include spike amplitudes within a percent (e.g., spk_detect_lb) of the maximum (e.g., spk_detect_ub). Thresholding also ensures accurate binning of motor activity spikes into bursts and collective fictive swim bouts. Generally, start with a threshold lower bound of 0.5, and gradually decrease until accurate detection is achieved.

For example, setting spk_detect_lb as 0.5 and spk_detect_ub as 1.0 will detect all spikes equal to or greater than 50% of the spike amplitude maximum and exclude noise or additional neurons of lower spike amplitudes (**Figure 2A**). Alternatively, one could also lower the spk_detect_ub from 1.0 to exclude neurons of higher spike amplitudes in order to isolate the neurons of lower spike amplitudes. Pre-processing figure outputs (see step 7.2.6) will inform whether adjustments and repeating from step 7.2.2 is necessary.

4. In the **Editor** window, click on **Run** to execute AffVR_preprocess.m.

5. Navigate to the previously converted .mat data file (see step 7.1.3); select and click on **Open** to begin automated preprocessing.

   NOTE: While the custom script is running, outputs will appear in the **Command Window** informing its progress through processing steps such as "filtering data …", "detecting ventral root activity …", and "generating figures …".

6. Figures generated by AffVR_preprocess.m will visualize afferent spike and VR detection and indicate whether any analysis variables should be adjusted (**Figure 2**).

7. Enter "Y" on the keyboard to save pre-processed metadata into a preprocess_output folder.

8. Pre-processed data will automatically output as **data_out.xls**.

3. Analyze the pre-processed data as desired.

Representative Results

After zebrafish larvae are properly immobilized and the posterior lateral line afferent ganglion and VR recording is achieved, activity in both afferent and motor neurons can be measured simultaneously. Recording channels are displayed using gap-free recording protocols (step 1.4) for continuous monitoring of afferent and VR activity. In real-time, decreases in spontaneous afferent spike rate can be observed concurrent with VR activity indicative of fictive swim bouts (**Figure 1E**). We found that best results and accurate spike detection were products of recordings that achieved a signal-to-noise ratio of at least 0.5. Custom written pre-processing scripts generate plots to assist in visualization of afferent and VR spike detection. Spontaneous afferent spikes are identified using a combination of spike parameters such as threshold, minimum duration (0.01 ms), and minimum inter-spike interval (ISI; 1 ms). Increasing negative pressure while establishing the recording often yields signal detection from multiple afferent units at once. Filtering by amplitude allows for distinguishing between signal dynamics of independent afferents. Isolating signals can be achieved by adjusting the lower-bound and upper-bound detection variables in the pre-processing script (**Figure 2A**). Aggressive suction to achieve multi-unit recordings can lead to unstable recordings, mechanical noise, degradation of afferent health, and ultimately a loss of signal. Therefore, it is important to slowly dial back suction to atmospheric pressure once the desired signal is achieved. Ventral root spike detection follows identical parameters to afferent spike detection but requires additional inputs to define distinct fictive swim bouts. Bursts within a motor command are defined by VR activity with a minimum of two spikes within 0.1 ms of each other and lasted a minimum of 5 ms. All swim bouts are

then delineated by a minimum of three bursts with inter-burst intervals of <200 ms (**Figure 2B**).

Afferent activity is difficult to interpret when looking at a recording in its entirety. Pre-processing scripts will overlay sections of afferent activity centered on a well-defined period of interest, in this case, the onset of a swim bout (n = 33, **Figure 2C**) to assist in visualizing trends in signal dynamics. Instantaneous afferent activity is calculated using a moving average filter and a 100 ms sampling window. Mean spontaneous activity shows dramatic changes in response to the onset of motor activity (**Figure 2C**). To better dissect and analyze afferent activity, periods before and after the swim are set to match the time interval of the corresponding swim bout. In the pre-processing script and representative analyzed results these periods are termed "pre-swim" and "post-swim". Pre-swim, swim, and post-swim spike rates were calculated by taking the number of spikes within the respective period over its duration. The precision of estimates for each individual is partly a function of the number of swims, so we analyzed variable relationships using weighted regressions, with individual weights equal to the square root of the number of swims.

Differences in afferent spike rates across the various periods of interest (pre-swim, swim, and post-swim) were tested by a two-way analysis of variance (ANOVA). Tukey's post-hoc test detected significant differences in spike rates between swimming spike rates and spike rates of both pre-swim (8.94 ± 0.2 Hz, relative decrease 57%) and post-swim (5.34 ± 0.2 Hz, relative decrease 40%) periods. The spike rate did not immediately return to the baseline given we also found that post-swim spike rate was lower than the pre-swim spike rate (Tukey post-hoc tests across groups, $p < 0.001$; **Figure 3A**). Linear models were used to detect relationships between relative spike rate and fictive swim parameters. Relative spike rate was calculated by taking the swim spike rate over the pre-swim spike rate. Fictive swim parameters included swim duration, swim frequency (i.e., number of bursts within a swim bout over the duration of the swim bout), and duty cycle (i.e., sum of the swim burst durations over the swim bout total duration). In our hands, the mean and variance of relative spike rate was correlated, so it was necessary for the data to be log transformed for analysis. Afferent spike rate was negatively correlated with swim duration meaning that the lateral line experiences greater inhibition during swims of longer duration ($r^2 = 0.186$, $F_{2,26} = 2.971$, $p = 0.045$; **Figure 3B**). There was no correlation detected between relative spike rate and neither swim frequency nor duty cycle (($r^2 = 0.099$, $F_{2,26} = 1.431$, $p = 0.231$, and $r^2 = 0.047$, $F_{2,26} = 0.645$, $p = 0.932$, respectively; **Figure 3C**,D). All analyses of variable relationships were weighted by the number of swims per individual and all the variables were then averaged by each individual (n = 29).

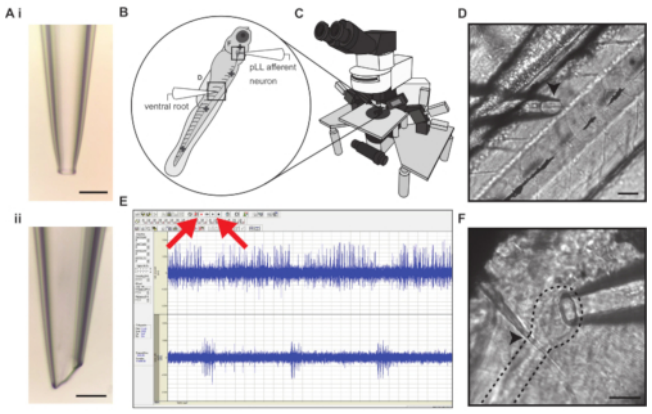

Figure 1: Simultaneous electrophysiological recording of posterior lateral line afferent neuron and ventral motor root activity. (**A**). Example of a loose-patch afferent (**i**) and ventral motor root (**ii**) recording electrodes. Scale bars represent 50 µm. (**B**) Larval zebrafish are paralyzed and pinned in four locations (cross symbols) to a Sylgard dish for recording stability. Bold crosses represent insertion points for pins. (**C**) The electrophysiology rig is mounted on a vibration-isolation table and consists of an upright fixed stage microscope on a motorized controller capable of 40x magnification. Dual current clamp and voltage clamp head stages are mounted on micromanipulators. (**D**) The myomeres of the body musculature are separated by myosepta that serve as recording landmarks for motor neuron arborizations. The ventral motor root electrode approaches the ventral body (left) and is centered and lowered on top of a myoseptum (arrowhead). Scale bar represents 50 µm. (**E**) Screen capture of electrophysiological recording in real-time allowing visualization of the spontaneous afferent activity (channel 1) and bursting ventral root activity indicative of fictive swim bout (channel 2). The Record and Play buttons are denoted with red arrows. (**F**) The posterior lateral line afferent ganglion (dashed line) lies just under the skin and can be identified by a tight cluster of afferent soma. The ganglion can be located by following the lateral line nerve past the cleithrum bone (arrowhead) to where it connects to the ganglion. Scale bar represents 30 µm. Please click here to view a larger version of this figure.

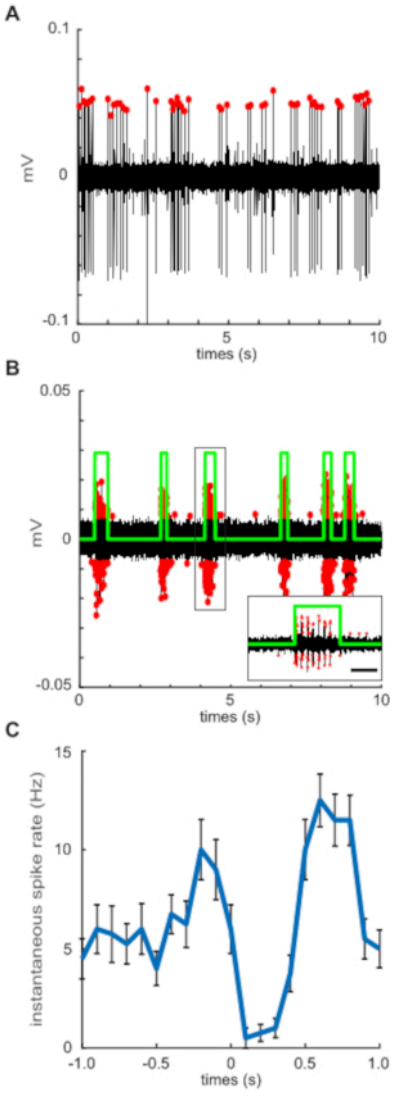

Figure 2: Pre-processing figure outputs visualize accurate spike detection. (**A**) Extracellular, loose-patch recording of posterior lateral line afferent neurons. Discrete spikes (labeled with red dots) are detected with a minimum inter-spike interval of 1 ms. Baseline noise and activity from other units are filtered out by thresholding to only include spike amplitudes within 50% of the maximum. (**B**) Ventral motor root recording (VR) of fictive swim bouts reveal voluntary motor commands throughout the duration of the recording. VR spikes (red dots) are detected using a similar threshold filter and then binned into a single swim bout (green) by detecting a burst of activity within 200 ms of one another (see insert; scale bar represents 200 ms). Spikes detected outside the defined swim bout do not occur within the inter-spike interval of stereotyped burst activity and are therefore excluded. (**C**) Mean spontaneous afferent spike rate centered on the onset of each swim bout (time = 0 s) illustrating spike rate before, during, and after swimming. Error bars represent ± SEM. Please click here to view a larger version of this figure.

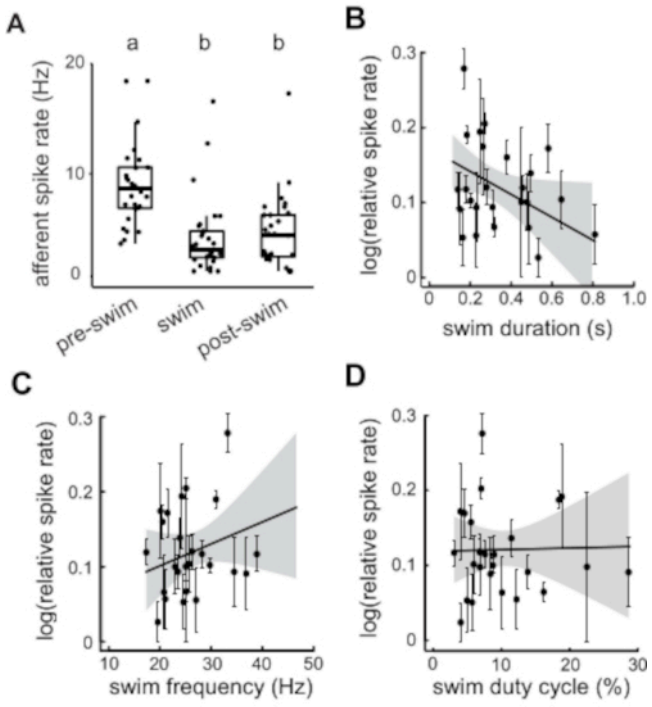

Figure 3: Quantification of afferent activity before, during, and after fictive swimming. (**A**) Afferent spike rate is significantly reduced during swimming and this effect persists even afterwards. Statistically similar groupings are denoted by a and b. (**B**) Longer swim duration is correlated to decreased afferent spike rate. **(C-D**) Swim frequency and swim duty cycle show no correlation to afferent spike rate. All values represent mean ± SEM. Outlying individuals with low statistical weight were omitted. Please click here to view a larger version of this figure.

Discussion

The experimental protocol described provides the potential to monitor endogenous changes in sensory input across motor behaviors in an intact, behaving vertebrate. Specifically, it details an in vivo approach to performing simultaneous extracellular recordings of lateral line afferent neurons and ventral motor roots in larval zebrafish. Spontaneous afferent activity has been previously characterized in zebrafish without consideration of potential concurrent motor activity[1,2,39,40,41]. Without monitoring the presence of motor activity with ventral root recordings, deciphering afferent activity will likely be underestimated due to the influence of efferent inhibition during, and even after, spontaneous swimming.

In vivo electrophysiological recordings are inherently challenging. In our experience, maintaining a healthy preparation is the single greatest factor to achieving successful, long-lasting recordings for afferent neurons and ventral motor roots. To do this, it is important to not only identify and monitor fast blood flow, but also recognize the texture of the skin and underlying musculature. We recommend observing several paralyzed larvae under a microscope before further handling to become familiar

with the intrinsic blood flow and skin state of healthy larvae. A successful ventral root recording through the skin requires a smooth, healthy skin surface in order for the recording electrode to generate a tight seal. This approach circumvents traditional protocols[37,42] that are invasive and time-consuming, which call for dissecting away the epithelium to expose the underlying musculature. An inconvenience of recording through the skin is the potential variability in time before signals are realized. Optimizing the magnitude and duration of applied negative pressure will decrease the time required to establish a signal and potentially improve the signal-to-noise ratio. Recordings from a healthy, active preparation should yield spontaneous afferent spike rates between 5-10 Hz with fictive swim bouts occurring every few seconds.

In addition to revealing motor activity state, ventral root recordings can serve as a proxy for monitoring efferent activity that discharges parallel to motor commands to attenuate lateral line activity[30,31,32] as well as activity in homologous hair cell systems (e.g., the auditory and vestibular system[35,43,44,45]). Efferent neurons reside deep in the hindbrain, making electrophysiological recordings of them exceedingly challenging. Zebrafish are a model genetic system, and our electrophysiology protocol can be complemented by transgenic lines to powerfully investigate aspects of corollary discharge, hair cell sensitivity, excitotoxicity, and beyond.

Disclosures

The authors declare no competing financial interests.

Acknowledgments

We gratefully acknowledge support from the National Institute of Health (DC010809), National Science Foundation (IOS1257150, 1856237), and the Whitney Laboratory for Marine Biosciences to J.C.L. We would like to thank past and present members of the Liao Lab for stimulating discussions.

References

1. Trapani, J. G., Nicolson, T. Mechanism of spontaneous activity in afferent neurons of the zebrafish lateral-line organ. *The Journal of Neuroscience.* **31** (5), 1614-1623 (2011).
2. Haehnel-Taguchi, M., Akanyeti, O., Liao, J. C. Afferent and motorneuron activity in response to single neuromast stimulation in the posterior lateral line of larval zebrafish. *Journal of Neurophysiology.* **112** (6), 1329-1339 (2014).
3. Levi, R., Akanyeti, O., Ballo, A., Liao, J. C. Frequency response properties of primary afferent neurons in the posterior lateral line system of larval zebrafish. *Journal of Neurophysiology.* **113** (2), 657-668 (2015).
4. Harris, G. G., Fishkopf, L. S., Flock, A. Receptor potentials from hair cells of the lateral line. *Science.* **167** (3914), 76-79. (1970).
5. Dow, E., Jacobo, A., Hossain, S., Siletti, K., Hudspeth, A. J. Connectomics of the zebrafish's lateral line neuromast reveals wiring and miswiring in a simple microcircuit. *eLife.* **7**, e33988 (2018).
6. Obholzer, N. et al. Vesicular glutamate transporter 3 is required for synaptic transmission in zebrafish hair cells. *The Journal of Neuroscience.* **28** (9), 2110-2118 (2008).
7. Keen, E. C., Hudspeth, A. J. Transfer characteristics of the hair cell's afferent synapse. *Proceedings of the National Academy of Sciences of the United States of America.* **103** (14), 5537-5542 (2006).

8. Li, G., Keen, E., Andor-Ardó, D., Hudspeth, A. J., von Gersdorff, H. The unitary event underlying multiquantal EPSCs at a hair cell's ribbon synapse. *The Journal of Neuroscience.* **29** (23), 7558-7568 (2009).
9. Manley, G. A., Robertson, D. Analysis of spontaneous activity of auditory neurons in the spiral ganglion of the guinea-pig cochlea. *The Journal of Physiology.* **258** (2), 323-336 (1976).
10. Kiang, N. Y. S., Watanabe, T., Thomas, E., Clark, L. *Discharge patterns of single fibers in the cat's auditory nerve.* MIT Press, Cambridge MA (1965).
11. Corey, D. P., Hudspeth, A. J. Ionic basis of the receptor potential in a vertebrate hair cell. *Nature.* **281** (5733), 675-677 (1979).
12. Trapani, J. G., Nicolson, T. Physiological recordings from zebrafish lateral-line hair cells and afferent neurons. *Methods in Cell Biology.* **100**, 219-231 (2010).
13. Reinig, S., Driever, W., Arrenberg, A. B. The descending diencephalic dopamine system is tuned to sensory stimuli. *Current Biology.* **27** (3), 318-333 (2017).
14. Zhang, Q. et al. Synaptically silent sensory hair cells in zebrafish are recruited after damage. *Nature Communications.* **9** (1), 1388 (2018).
15. Pichler, P., Lagnado, L. Motor behavior selectively inhibits hair cells activated forward motion in the lateral line of zebrafish. *Current Biology.* ***30***. (1), 150-157 (2020).
16. Olszewski, J., Haehnel, M., Taguchi, M., Liao, J. C. Zebrafish larvae exhibit rheotaxis and can escape a continuous suction source using their lateral line. *PloS One.* **7** (5), e36661 (2012).
17. Suli, A., Watson, G. M., Rubel, E. W., Raible, D. W. Rheotaxis in larval zebrafish is mediated by lateral line mechanosensory hair cells. *PLoS One.* **7** (2), e29727 (2012).
18. Oteiza, P., Odstcil, I., Lauder, G., Portugues, R., Engert, F. A novel mechanism for mechanosensory-based rheotaxis in larval zebrafish. *Nature.* **547** (7664), 445-448 (2017).
19. McHenry, M. J., Feitl, K. E., Strother, J. A. Larval zebrafish rapidly sense the water flow of a predator's strike. *Biology Letters.* **5** (4), 477-479 (2009).
20. Stewart, W. J., Cardenas, G. S., McHenry, M. J. Zebrafish larvae evade predators by sensing water flow. *The Journal of Experimental Biology.* **216** (Pt 3), 388-398 (2013).
21. Mekdara, P. J., Schwalbe, M. A. B., Coughlin, L. L., Tytell, E. D. The effects of lateral line ablation and regeneration in schooling giant danios. *The Journal of Experimental Biology.* **221** (Pt 8), 175166 (2018).
22. Palmer, L. M., Giuffrida, B. A., Mensinger, A. F. Neural recordings from the lateral line in free-swimming toadfish, *Opsanus tau. The Biological Bulletin.* **205** (2), 216-218 (2003).
23. Ayali, A., Gelman, S., Tytell, E. D., Cohen, A. H. Lateral line activity during undulatory body motions suggests a feedback link in closed-loop control of sea lamprey swimming. *Canadian Journal of Zoology.* **87** (8), 671-683 (2009).
24. Mensinger, A. F., Van Wert, J. C., Rogers, L. S. Lateral line sensitivity in free-swimming toad fish Opsanus tau. *The Journal of Experimental Biology.* **222** (Pt 2), 190587 (2019).

25. Montgomery, J., Bodznick, D., Halstead, M. Hindbrain signal processing in the lateral line system of the dwarf scorpionfish *Scopeana papillosus. The Journal of Experimental Biology.* **199** (Pt 4), 893-899 (1996).
26. Montgomery, J. C., Bodznick, D. An adaptive filter that cancels self-induced noise in the electrosensory and lateral line mechanosensory systems of fish. *Neuroscience Letters.* **174** (2), 145-148 (1994).
27. Palmer, L. M., Deffenbaugh, M., Mensinger, A. F. Sensitivity of the anterior lateral line to natural stimuli in the oyster toadfish, *Opsanus tau* (Linnaeus). *The Journal of Experimental Biology.* **208** (Pt 18), 3441-3450 (2005).
28. Russell, I. J., Roberts, B. L. Inhibition of spontaneous lateral-line activity of efferent nerve stimulation. *The Journal of Experimental Biology.* **57**, 77-82 (1972).
29. Lunsford, E. T., Skandalis, D. A., Liao, J. C. Efferent modulation of spontaneous lateral line activity during and after zebrafish motor commands. *Journal of Neurophysiology.* ***122***. (6), 2438-2448 (2019).
30. Russell, I. J. The pharmacology of efferent synapses in the lateral-line system of *Xenopus laevis. The Journal of Experimental Biology.* **54** (3), 643-659 (1971).
31. Roberts, B. L., Russell, I. J. The activity of lateral-line efferent neurons in stationary and swimming dogfish. *The Journal of Experimental Biology.* **57** (2), 435-448 (1972).
32. Flock, A., Russell, I. J. The post-synaptic action of efferent fibres in the lateral line organ of the burbot *Lota lota. The Journal of Physiology.* **235** (3), 591-605 (1973).
33. Montgomery, J. C. Noise cancellation in the electrosensory system of the thornback ray; common mode rejection of input produced by the animal's own ventilatory movement. *Journal of Comparative Physiology.* **155**, 103-111 (1984).
34. Tricas, T. C., Highstein, S. M. Action of the octavolateralis efferent system upon the lateral line of free-swimming toadfish, *Opsanus tau. Journal of Comparative Physiology.* **169** (1), 25-37 (1991).
35. Weeg, M. S., Land, B. R., Bass, A. H. Vocal pathways modulate efferent neurons to the inner ear and lateral line. *The Journal of Neuroscience.* **25** (25), 5967-5974 (2005).
36. Elgoyhen, A. B., Johnson, D. S., Boulter, J., Vetter, D. E., Heinemann, S. α9: an acetylcholine receptor with novel pharmacological properties expressed in rat cochlear hair cells. *Cell.* **79** (4), 705-715 (1994).
37. Masino, M. A., Fetcho, J. R. Fictive swimming motor patterns in wild type and mutant larval zebrafish. *Journal of Neurophysiology.* **93** (6), 3177-3188. (2005).
38. Hentschke, H. abfload. *MATLAB Central File Exchange.* 1.4.0.0. (2020).
39. Harris, G. G., Milne, D. C. Input-output characteristics of the lateral-line sense organs of *Xenopus laevis. The Journal of the Acoustical Society of America.* **40** (1), 32-42 (1966).
40. Liao, J. C., Haehnel, M. Physiology of afferent neurons in larval zebrafish provides a functional framework for lateral line somatotopy. *Journal of Neurophysiology.* **107** (10), 2615-2623 (2012).
41. Song, S. et al. Mathematical modeling and analyses of interspike-intervals of spontaneous activity in afferent neurons of the zebrafish lateral line. *Nature Science Reports.* **8**, 14851 (2018).

42. Liao, J. C., Fetcho, J. R. Shared versus specialized glycinergic spinal interneurons in axial motor circuits of larval zebrafish. *The Journal of Neuroscience.* **28** (48), 12982-12992 (2008).

43. Holst, E. von, Mittelstaedt, H. The principle of reafference: interactions between the central nervous system and the peripheral organs. *Die Naturwissenschften.* **37**, 463-576 (1950).

44. Crapse, T. B., Sommer, M. A. Corollary discharge across the animal kingdom. *Nature Reviews. Neuroscience.* **9** (8), 587-600 (2008).

45. Brichta, A. M., Goldberg, J. M. Responses to efferent activation and excitatory response-intensity relations of turtle posterior-crista afferents. *Journal of Neurophysiology.* **83** (3), 1224-1242 (2000).